Electronic Supplementary Material (ESI) for Journal of Materials Chemistry C.

Two-Dimensional Janus Monolayers Al_2XYZ (X/Y/Z = S, Se, Te, X≠Y≠Z): First-principles Insight onto the Photocatalytic and Highly Adjustable Piezoelectric Properties

Chenchen Qi[a], Cuixia Yan[a]*(Equal contribution), Qiuyang Li[a], Ting Yang[a], Shi Qiu[a], Jinming Cai[a]

a. Faculty of Materials Science and Engineering, Kunming University of Science and Technology, Kunming, 650093, People's Republic of China

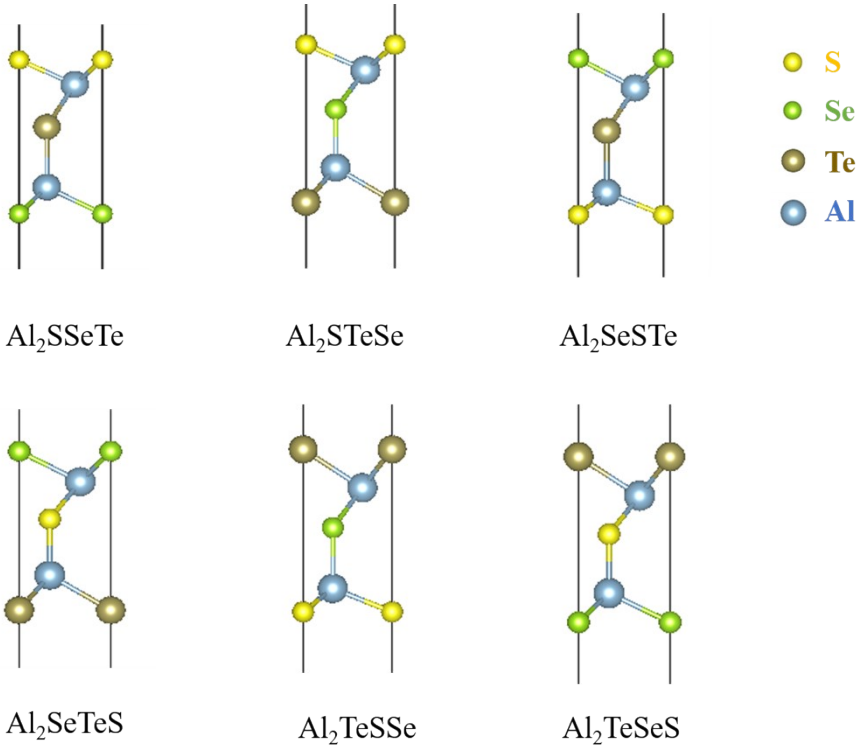

Figure S1. *Six models of Al_2XYZ (X/Y/Z = S, Se, Te, X≠Y≠Z) monolayers (Al_2SSeTe, Al_2STeSe, Al_2SeSTe, Al_2SeTeS, Al_2TeSSe, and Al_2TeSeS). Dark blue, yellow, green and brown balls refer to the Al, S, Se and Te atoms, respectively.*

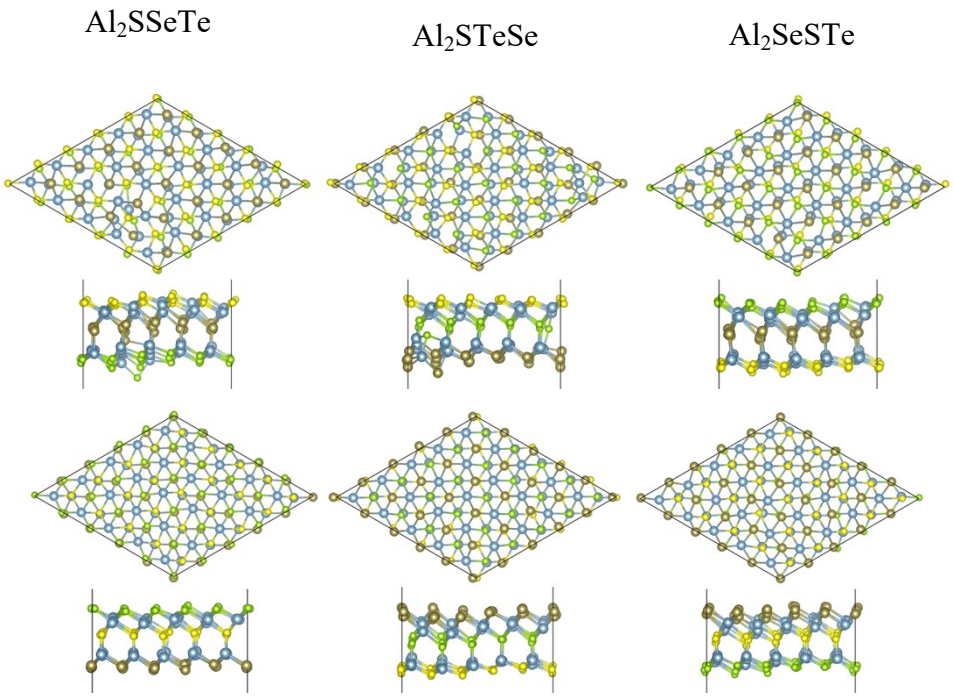

Figure S2. *Top and side views of the snapshots of the six geometric structure of Al_2XYZ (X/Y/Z = S, Se, Te, X≠Y≠Z) monolayers taken form ab initio molecular dynamics (AIMD) simulation carried out at 300 K for 5 ps.*

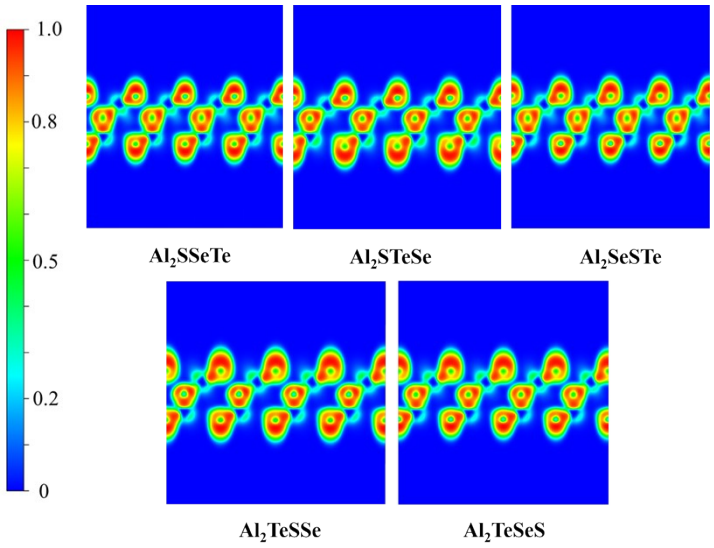

Figure S3. *The corresponding ELF of Al_2SSeTe, Al_2STeSe, Al_2SeSTe, Al_2TeSSe, and Al_2TeSeS monolayers. (The values of vertical bar represent the localized level of electrons. The values of 0.0, 0.5 and 1.0 represent fully delocalized, electron–gas-like pair probability and entirely localized electrons, respectively.)*

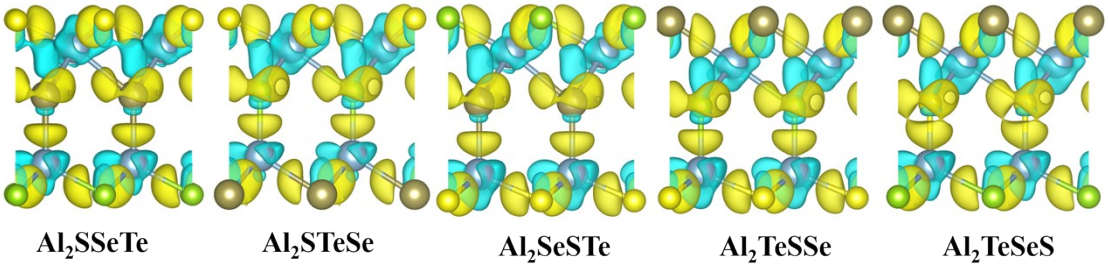

Figure S4. *Charge density differences of Al_2SSeTe, Al_2STeSe, Al_2SeSTe, Al_2TeSSe, and Al_2TeSeS monolayers. (The light blue and yellow represent the electron depletion and electron accumulation in the surface of 0.005 e/Å3, respectively. The sections of electron density clouds are also represented.)*

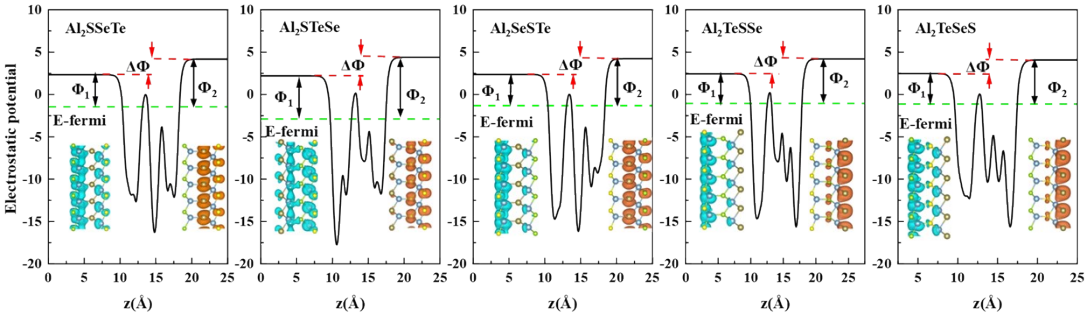

Figure S5. *Plane-averaged electrostatic potential and partial charge density of Al_2SSeTe, Al_2STeSe, Al_2SeSTe, Al_2TeSSe, and Al_2TeSeS monolayers.*

Table S1. *The in-plane/out-plane piezoelectric stress coefficients e_{11}/e_{31}, in-plane/out-of-plane piezoelectric coefficient d_{11}/d_{31} of Al_2XYZ (X/Y/Z = S, Se, Te, X≠Y≠Z)* monolayers.

	$e_{11}(10^{-10}C/m)$	$e_{31}(10^{-10}C/m)$	$d_{11}(pm/V)$	$d_{31}(pm/V)$
Al_2SSeTe	2.71	0.39	3.93	0.28
Al_2STeSe	2.12	0.39	3.46	0.32
Al_2SeSTe	12.22	0.21	19.24	0.16
Al_2SeTeS	10.00	0.07	41.28	0.07
Al_2TeSSe	5.89	0.26	11.18	0.21
Al_2TeSeS	11.82	0.15	29.85	0.14

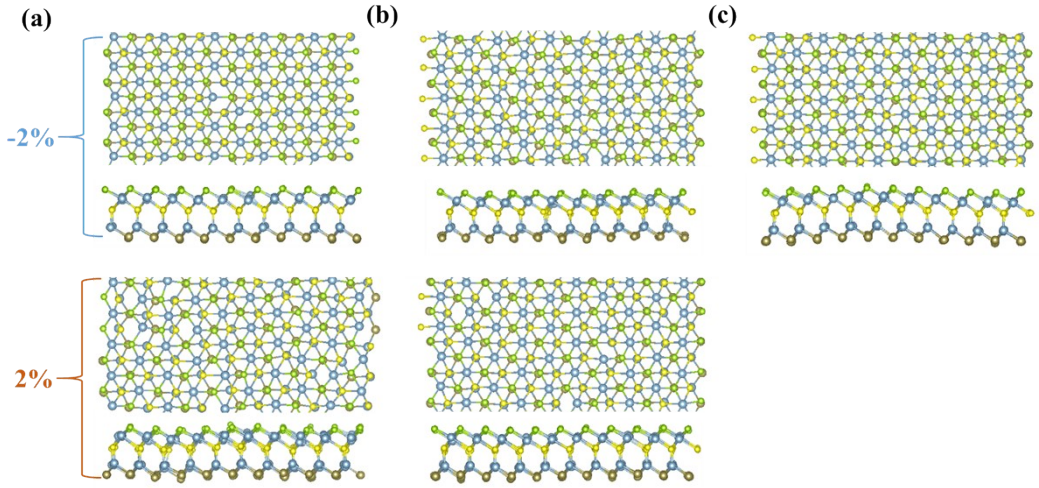

Figure S6. *Top and side views of the snapshots of Al_2SeTeS monolayer* at 2% and -2% *uniaxial (along (a) the x-axis and (b) y-axis) and (c) biaxial strain taken form ab initio molecular dynamics (AIMD) simulation carried out at 300 K for 5 ps.*

Table S2. *The elastic stiffness constants (C_{ij}) and piezoelectric coefficients (e_{ij}/d_{ij}) in Al_2SeTeS monolayer under the effect of uniaxial strains along the x-direction.*

$Al_2STeSe(x)$	Eg(eV)/x	$C_{11}(N/m)$	$C_{12}(N/m)$	$e_{11}(10^{-10}C/m)$	$e_{31}(10^{-10}C/m)$	$d_{11}(pm/V)$	$d_{31}(pm/V)$
-2%	1.65(ID)	89.48	33.60	2.46	0.22	4.40	0.18
-1.5%	1.71(ID)	85.03	35.77	4.07	0.20	8.26	0.17
-1%	1.79(ID)	81.10	37.39	5.31	0.19	12.15	0.16
-0.5%	1.83(D)	71.57	41.72	8.61	0.08	28.86	0.07
0%	2.14(ID)	67.34	43.11	10.00	0.07	41.27	0.06
0.5%	1.87(ID)	61.89	44.35	11.84	0.04	67.51	0.04
1%	1.86(ID)	51.87	46.46	14.61	0.15	270.04	0.15
1.5%	1.83(ID)	48.53	44.81	15.10	0.22	405.63	0.24
2%	1.82(ID)	48.04	41.88	14.61	0.23	237.52	0.25

Table S3. *The elastic stiffness constants (C_{ij}) and piezoelectric coefficients (e_{ij}/d_{ij}) in*

Al_2SeTeS monolayer under the effect of uniaxial strains along the y-direction.

Al_2STeSe(y)	Eg(eV)/y	C_{11}(N/m)	C_{12}(N/m)	e_{11}(10^{-10}C/m)	e_{31}(10^{-10}C/m)	d_{11}(pm/V)	d_{31}(pm/V)
-2%	1.73(ID)	51.99	40.50	13.98	0.22	121.72	0.24
-1.5%	1.78(ID)	50.95	44.18	15.10	0.22	222.81	0.23
-1%	1.82(ID)	54.81	45.72	13.77	0.12	151.48	0.12
-0.5%	1.85(ID)	61.10	44.71	11.97	0.02	73.05	0.02
0%	2.14(ID)	67.34	43.11	10.00	0.07	41.27	0.06
0.5%	1 .86(D)	68.92	42.49	9.10	0.08	34.45	0.07
1%	1.83(ID)	76.93	38.82	6.39	0.18	16.76	0.16
1.5%	1.79(ID)	81.42	36.42	4.70	0.22	10.45	0.19
2%	1.75(D)	84.65	33.91	3.21	0.24	6.33	0.20

Table S4. *The elastic stiffness constants (C_{ij}) and piezoelectric coefficients (e_{ij}/d_{ij}) in Al_2SeTeS monolayer under the effect of biaxial strains.*

Al_2STeSe(xy)	Eg(eV)/xy	C_{11}(N/m)	C_{12}(N/m)	e_{11}(10^{-10}C/m)	e_{31}(10^{-10}C/m)	d_{11}(pm/V)	d_{31}(pm/V)
-2%	1.89	84.93	38.74	6.35	0.10	13.74	0.08
-1.5%	1.97	80.72	39.43	7.08	0.09	17.14	0.08
-1%	2.03	76.26	40.45	7.97	0.08	22.27	0.07
-0.5%	2.10	71.88	41.52	8.86	0.07	29.18	0.07
0%	2.14	67.34	43.11	10.00	0.07	41.28	0.06
0.5%	2.13	62.37	44.79	11.16	0.06	63.48	0.06
1%	2.11	57.69	46.46	12.33	0.05	109.82	0.05
1.5%	2.09	52.47	48.78	13.77	0.05	373.13	0.05
2%	2.07	47.88	50.55	-	-	-	-

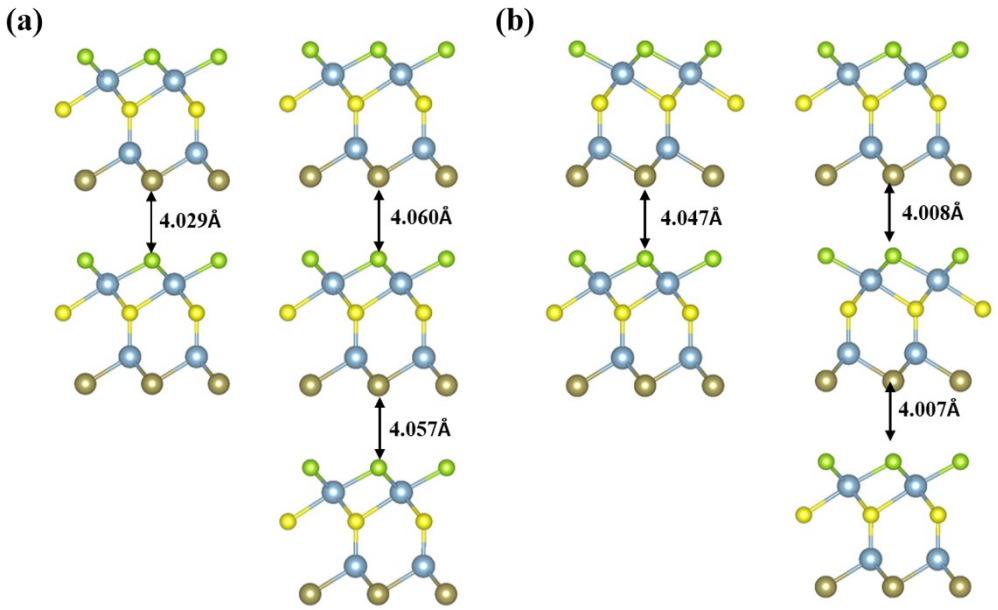

Figure S7. *The 2D Al_2SeTeS multilayer structure of two-layer, three-layer Al_2SeTeS monolayer stacked in AA (a) and AB (b) mode.*

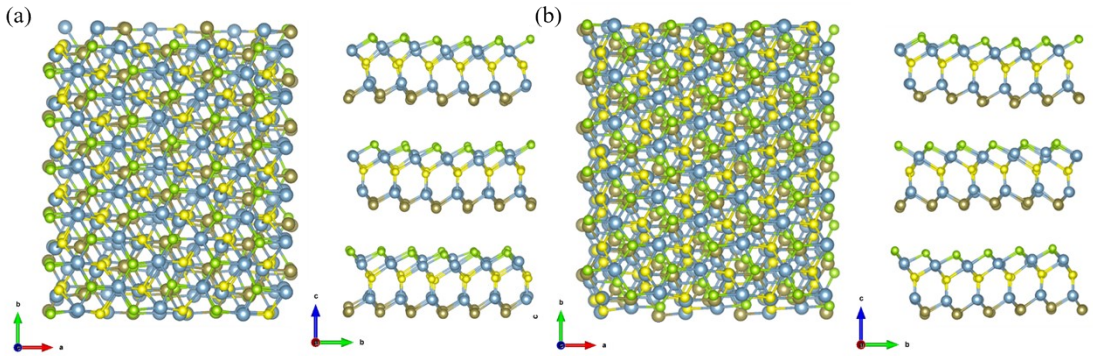

Figure S8. *Top and side views of the snapshots of three-layer Al_2SeTeS monolayer stacked in (a) AA and (b) AB mode taken form ab initio molecular dynamics (AIMD) simulation carried out at 300 K for 5 ps.*

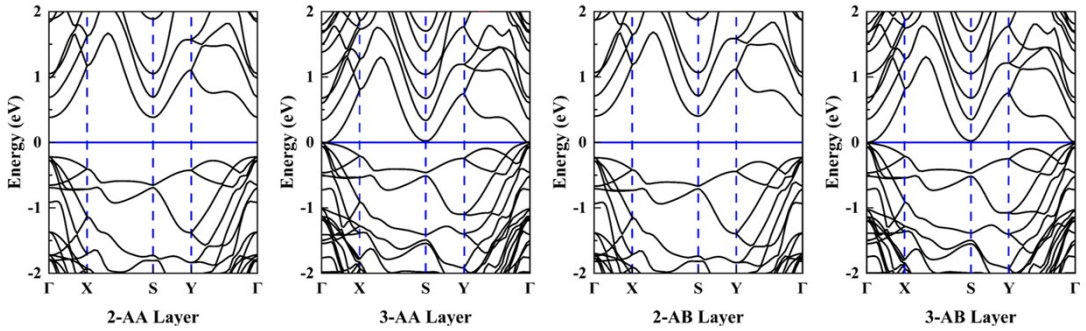

Figure S9. *The band of two-layer and three-layer Al_2SeTeS stacked in AA and AB mode.*

Table S5. *The formation energies (E_f), band gap (E_g), elastic stiffness constants (C_{ij}) and piezoelectric coefficients (e_{ij}/d_{ij}) in two-layer, three-layer Al_2SeTeS stacked in AA and AB mode.*

Al_2STeSe		E_f(eV)	Eg(eV)	C_{11}(N/m)	C_{12}(N/m)	e_{11}(10^{-10}C/m)	e_{31}(10^{-10}C/m)	d_{11}(pm/V)	d_{31}(pm/V)
AA	2	-0.35	0.60(D)	118.91	68.44	13.74	0.05	27.23	0.028
	3	-0.73	0.05(D)	117.56	71.93	18.14	0.21	39.75	0.11
AB	2	-0.35	0.63(D)	126.14	69.58	0.15	0.87	0.27	0.44
	3	-0.74	0.08(D)	140.44	81.36	3.51	0.59	5.95	0.27